

An Intelligent Approach to Prognostic Enhancements of Diagnostic Systems

George Vachtsevanos^{*a}, Peng Wang^{*a}, Noppadon Khiripet^{*a}, Ash Thakker^{**b}, Thomas Galie^{***c}
^aGeorgia Institute of Technology; ^bGlobal Technology; ^cPhiladelphia Naval Business Center

ABSTRACT

This paper introduces a novel methodology to prognostics based on a dynamic wavelet neural network construct and notions from the virtual sensor area. This research has been motivated and supported by the U.S. Navy's active interest in integrating advanced diagnostic and prognostic algorithms in existing Naval digital control and monitoring systems. A rudimentary diagnostic platform is assumed to be available providing timely information about incipient or impending failure conditions. We focus on the development of a prognostic algorithm capable of predicting accurately and reliably the remaining useful lifetime of a failing machine or component. The prognostic module consists of a virtual sensor and a dynamic wavelet neural network as the predictor. The virtual sensor employs process data to map real measurements into difficult to monitor fault quantities. The prognosticator uses a dynamic wavelet neural network as a nonlinear predictor. Means to manage uncertainty and performance metrics are suggested for comparison purposes. An interface to an available shipboard Integrated Condition Assessment System is described and applications to shipboard equipment are discussed. Typical results from pump failures are presented to illustrate the effectiveness of the methodology.

Keyword: prognosis, virtual sensor, dynamic wavelet neural network

1. INTRODUCTION

Condition-based maintenance (CBM) typically entails a diagnostic module which detects and identifies incipient component or subsystem failure conditions, a prognostic module whose task is to estimate the remaining useful lifetime of the failing component and a maintenance scheduler which schedules maintenance in order to maximize equipment uptime while meeting certain constraints.

This paper addresses issues relating to the prognostic module – the Achilles heel of the CBM architecture. Fault diagnosis is a mature field with contributions ranging from model-based techniques to data-driven configurations that capitalize upon soft computing and other “intelligent” tools (Konrad & Isermann 1996, Mylaraswamy & Venkatasubramanian 1997). CBM scheduling is a complex task that involves finding the “optimum” time to perform maintenance within the window prescribed by the Prognosticator while meeting a host of constraints. This scheduling problem may be formulated as a multi-objective optimization problem where the main objective is to maximize process uptime while satisfying a set of constraints that relate to resource and maintenance personnel availability, production and scheduling requirements, redundant or relocatable machines, timing constraints, etc (Barbera et al 1996, Makis et al 1998, Prickett & Eavery 1991). The word “prognosis” implies the foretelling of the probable course of a disease (Taylor 1953), a term widely used in medical practice. In the industrial and manufacturing arenas, prognosis is interpreted to answer the question: what is the remaining useful lifetime of a machine or a component once an impending failure condition is detected and identified? Stochastic Auto-Regressive Integrated Moving Average (ARIMA) models (Jardim-Goncalves et al 1996), fuzzy pattern recognition principles (Frelicot 1996), knowledge-intensive expert systems (Lembessis et al 1989), nonlinear stochastic models of fatigue crack dynamics (Ray & Tangirala 1994), polynomial neural networks (Parker et al 1993), Weibull models (Groer 2000), and other techniques have been introduced over the past years to address the diagnostic/prognostic problem. This paper attempts to address this issue by introducing a novel combination of a “virtual” sensor as a mapping tool between known measurements and “difficult-to-access” quantities and a dynamic wavelet neural network as the “predictor”, i.e. the construct that projects into the future the temporal behavior of a faulted component.

* gjv@ee.gatech.edu; (404)894-6252 Voice; (404)894-7583 Fax; <http://icsl.marc.gatech.edu>; Georgia Institute of Technology; School of Electrical & Computer Engineering; Atlanta GA 30332-0250; ** globaltech.conexn@att.net; (770)971-4084 Voice; (770)971-1846 Fax; Global Technology; 2690 Spencer's Trace, #108; Marietta, GA 30062; *** galiert@nswccd.navy.mil; (215)897-7960 Voice; (215)897-7600 Fax; Naval Surface Warfare Center, Carderock Division; Philadelphia Naval Business Center; Philadelphia PA 19112-5083

2. PROGNOSTICATION

Prognosticators perform the vital function of linking the diagnostic information with the maintenance scheduler. They are probably the least understood but most crucial component of the diagnostic/prognostic/CBM hierarchical architecture. Furthermore, they entail ambiguity and large-grain uncertainty since the historical evolution of a failure event – the growth of a structural fault, for example – is difficult if not impossible to model accurately, historical data is not readily available and the particular growth phenomenon may be strongly dependent on the system structure, operating conditions, environmental effects, etc. They are viewed as dynamic predictors that receive fault data from the diagnostic module and determine the allowable time window during which machine maintenance must be performed if the integrity of the process is to be kept as high as possible. The term “dynamic predictor” implies also the functional requirement that the target output, i.e. remaining useful lifetime or time-to-failure, is dynamically updated as more information becomes available from the diagnostician. Thus, this scheme should reduce the uncertainty and improve the prediction accuracy as the accumulated evidence grows. Figure 1 depicts the overall architecture of the proposed prognostic system. The diagnostician monitors continuously critical sensor data and decides upon the existence of impending or incipient failure conditions. The detection and identification of an impending failure triggers the prognosticator. The latter reports to the CBM module primarily the remaining useful lifetime of the failing machine or component. The CBM module schedules the maintenance so that uptime is maximized while certain constraints are satisfied. The schematic of Figure 1 focuses on the functionalities of the prognosticator. The diagnostician alerts the prognostic module and provides failure and other pertinent sensor data to it. The prognostic architecture is based on two constructs: a static “virtual sensor” that relates known measurements to fault data and a predictor which attempts to project the current state of the faulted component into the future thus revealing the time evolution of the failure mode and allowing the estimation of the component’s remaining useful lifetime. Both constructs rely upon a Wavelet Neural Network (WNN) model acting as the mapping tool.

2.1 Wavelet Neural Networks

WNNs belong to a new class of neural networks with unique capabilities in addressing identification and classification problems. Wavelets are a class of basic elements with oscillations of effectively finite-duration that makes them like “little waves”. The self-similar, multiple resolution nature of wavelets offers a natural framework for the analysis of physical signals and images. On the other hand, artificial neural networks constitute a powerful class of nonlinear function approximants for model-free estimation. A common ground between these two technologies may be coherently exploited by introducing a WNN. Indeed, the implementation of a neural network is closely related to a truncated version of the wavelet series.

A multi-input multi-output (MIMO) WNN is illustrated in Figure 2, which has only one hidden layer. This WNN can be formulated, in a vector format, as (Schauz 1996):

$$y = [\psi_{A_1, b_1}(x) \ \psi_{A_2, b_2}(x) \ \cdots \ \psi_{A_M, b_M}(x)]C + [x \ 1]C_{lin} \quad (1)$$

where x is the $1 \times n$ input row-vector; y is the $1 \times K$ output row-vector and K is the number of outputs; A_j is the $n \times n$ squashing matrix for the j th node; b_j is the $1 \times n$ translation vector for the j th node; C is the $M \times K$ matrix of output coefficients, where M is the number of wavelet nodes; C_{lin} is the $(n+1) \times K$ matrix of output coefficients for the linear direct link; and ψ is the wavelet function that can take the form:

$$\psi_{A,b}(x) = |A|^{1/4} \psi(\sqrt{(x-b)A(x-b)^T}) \quad (2)$$

where x is the input row-vector; A the squashing matrix for the wavelet; b the translation vector; and T the transpose operator. Composed of localized basis functions, the WNNs are suitable for capturing the local nature of the data patterns and thus are efficient tools for both classification and approximation problems.

Equation (1) is a static model in the sense that it establishes a static relation between its inputs and outputs. All signals flow in a forward direction only with this configuration. Dynamic or recurrent neural networks, on the other hand, are required to model the time evolution of dynamic systems. Signals in such a network configuration can flow not only in the forward direction but also can propagate backwards, in a feedback sense, from the output to the input nodes. Dynamic wavelet neural nets have recently been proposed to address the prediction/classification issues. A multi-resolution dynamic predictor that utilizes the discrete wavelet transform and recurrent neural networks forming nonlinear models for prediction was designed and employed for multi-step prediction of the intra-cranial pressure signal (Tsui et al 1995). A recurrent wavelet neural

network was developed for the blind equalization of nonlinear communication channels (He & He 1997); recurrent wavelet neural networks were also derived by Rao & Kumthekar (1994) using the real-time Back-Propagation (BP) algorithm.

The basic structure of a DWNN is shown in Figure 3. Delayed versions of the input and output augment now the input feature vector and the resulting construct can be formulated as:

$$Y(t+1) = WNN(Y(t), \dots, Y(t-M), U(t), \dots, U(t-N)) \quad (3)$$

where U is the external input; Y is the output; M is the number of outputs minus 1; N is the number of external inputs minus 1; and WNN stands for a static WNN. When measuring the angular velocity of a servo motor, for example, Y(t) could be the velocity to be measured and U(t) be the regulating voltage that controls the motor's rotation at time t. Equation (3) forms an evolving or prediction model that dynamically maps the historical and current data into the future. In essence, this DWNN is a kind of partially recurrent WNNs of simple but well-defined structures that are more convenient to design and apply in practical situations than the fully recurrent WNNs. Compared to traditional prediction techniques such as ARIMA, DWNNs offer, in a systematic manner, more flexibility in terms of nonlinear mapping, parallel processing, heuristics-based learning, and hardware implementation.

2.2 Virtual Sensors

It is often true that machine or component faults are not directly accessible for monitoring their growth behavioral patterns. Consider, for example, the case of a bearing fault. No direct measurement of the crack dimensions is possible when the bearing is in an operational state. That is, there is no such device as a "fault meter" capable of providing direct measurements of the fault evolution. Examples of a similar nature abound. Marko et al (1996) developed a neural net-based virtual or ideal sensor used to diagnose engine combustion failures, known as misfire detection. Their technique employs a recurrent neural net as the classifier that takes such inputs as crankshaft acceleration, engine speed, engine load and engine ID and produces a misfire diagnostic evaluation as the output. In the present study, the same concept is exploited to design a virtual sensor which takes as inputs measurable quantities or features and outputs the time evolution of the fault pattern. A schematic representation of such a WNN as a virtual sensor is illustrated in Figure 4.

2.3 Predictors

A fault predictor based on the DWNN is shown in Figure 5. The process is monitored real-time using appropriate sensors. Here, virtual sensors can also be employed to measure signals or their derivatives that are difficult to record on-line and on-site. Data obtained from measurements are continuously processed and features extracted on a time scale. The features are organized into a time-stamped feature vector that serves as the input to the DWNN. Consequently, the DWNN performs as a dynamic classifier or identifier. The data used to train the predictor must be recorded with time information, which is the basis for the prognosis-oriented prediction task. In the case of a bearing fault, the predictor could take the fault dimensions, failure rates, trending information, temperature, component ID, etc. as its inputs and generate the fault growth as the output. Feature extraction can be performed periodically for the processes under prognosis. It should be noted that features are extracted in temporal series and are dynamic in the sense that the DWNN processes them in a dynamic fashion. Then, the obtained features are fused into the time-dependent feature vector that characterizes the process at the designated time instants. Feature selection is based on criteria that distinguish a fault signature from normal operating conditions and one particular fault mode from another. Such other criteria as computational cost may be included.

The DWNN must be trained and validated before any on-line implementation and use. Such algorithms as the Back-Propagation or GA can be used to train the network. Once trained, the DWNN, along with the TTF calculation mechanism, can act as an on-line prognostic operator. It is worth reiterating that the results from the diagnosis serve as the input to the prognosis. Thus, the fidelity and accuracy of the diagnostician bears a direct impact on the reliability of the prognosticator. Predictions can be substantially improved as more fault data become available. The diagnostic/prognostic operation is viewed, therefore, as a dynamic, "evolving" mechanism with adaptive observation and prediction windows. More accurate predictions can result from the utility of additional historical information. The DWNN is, indeed, updated on-line in a real-time fashion.

3. UNCERTAINTY MANAGEMENT

Uncertainty representation and management for fault prognosis are difficult tasks since prognosis involves both subjective and objective uncertainties and operates over the time horizon from the past, through the present and to the future. Uncertainty sources must be identified and modeled. Uncertainty management schemes, i.e., methods to reduce the

uncertainty bounds as more data becomes available, must be derived. Probability and possibility theories are two candidates of mathematical tools to deal with these issues.

For simplicity, this paper deals only with data uncertainties and uses uncertainty boundaries for reporting prognostic results. This results in the so-called interval predictions, compared to point predictions. An uncertainty interval can be generated through the estimation of a lower and an upper bound of the prediction window. As shown in Figure 6, a fault indicated by the feature $F(t)$ would evolve along its mean $F_M(t)$ and within its lower bound $F_L(t)$ and upper bound $F_U(t)$. Hence, the fault prognosis problem can be stated as: using historic data of $F(t)$ to predict its mean $F_M(t)$ and boundaries $[F_L(t) F_U(t)]$ until the remaining useful lifetime or the time-to-failure of the targeted component is found with its mean T_M and confidence interval $[T_L T_U]$, under a certain failure criterion F_F . For example, a faulty servomotor could be prognosticated as having a remaining useful lifetime of around 15 hours, probably between 10 and 20 hours, under the criterion that the temperature of the motor should not exceed 70°C . In this case, $T_M = 15$ days, $T_L = 10$ days, $T_U = 20$ days, and $F_F = 70^\circ\text{C}$.

Generally, $F_M(t)$, $F_L(t)$, and $F_U(t)$ can be obtained by applying statistical or fuzzy clustering techniques to the given data. The mean $F_M(t)$ is the center of the data points at the time instant t . The lower bound $F_L(t)$ is the smallest data point at the time instant t . The upper bound $F_U(t)$ is the largest data point at the time instant t . The upper bound $F_U(t)$ and the lower bound $F_L(t)$ harness the development of the mean $F_M(t)$ so that the instantaneous feature $F(t)$ should appear to be moving in a band. However, it is not very applicable to allow $F_U(t)$ and $F_L(t)$ to be the extreme data points that are much less populated. A better way is to choose $F_U(t)$ and $F_L(t)$ using a confidence level, say, α to trim the probability density function (PDF) of $F(t)$, as shown in Figure 7.

4. PERFORMANCE ASSESSMENT

When a number of prognostic algorithms are available for a certain prognostic task, it is essential to compare these algorithms and select the best one for implementation so that the prognosis can be accomplished in a more efficient and effective manner. For example, how to rate a DWNN based prognosticator against a traditional auto-regression (AR) based one for the targeted application. It is essential, therefore, that means are devised to assess the performance of various prognostic algorithms. In general, an assessment methodology should consider both the technical and economic feasibility of the algorithms and their associated implementation platforms. Consequently, performance measures (PMs) should include the cost of equipment and maintenance, personnel expenses, accuracy of detection and prediction, etc, which are usually grouped into two categories: those associated with economic factors and the ones relating to the technical (or algorithmic) concerns. In the second, accuracy, speed, complexity and scalability are typical measures, whereas the first includes purchase and implementation costs, maintainability, computing resources, reliability, user-friendliness, among others.

5. AN ILLUSTRATIVE EXAMPLE

Industrial chillers are typical processes found in many critical applications. These devices support electronics, communications, etc. on a navy ship, computing and communication in commercial enterprises, refrigeration and other functions in food processing, etc. Of special interest is the fact that their design incorporates a diverse assemblage of common and vital components, i.e. pumps, motors, compressors, etc. A rich variety of failure modes are observed on such equipment ranging from vibration-induced faults to electrical failures and a multitude of process-related failure events. Most chillers are well instrumented monitoring vibrations, temperature, pressure, flow, etc., and many mechanical faults exhibit symptoms that are sensed via vibration measurements. For example, a water pump will vibrate if its motor bearing is defective, if its shaft is misaligned or if its mounting is somewhat loose. A rolling-element bearing fault is used in this study to demonstrate the feasibility of the prognostic algorithms.

Defective bearings or loose mounting bolts would cause pumps to vibrate abnormally. The vibrations are typically monitored by accelerometers with the measured signals transferred to data acquisition units via co-axial cables. Shiroishi et al (1997) collected tri-axial vibration signals originating from a bearing with a crack in its inner race. An initial crack was seeded in the bearing and the experiment was run for a period of time and vibration data were recorded during that period. The set-up was then stopped and the crack size was increased followed by a second run. This procedure was repeated until the bearing failed. The crack sizes were organized in an ascending order while time information was assumed uniformly distributed among the crack sizes. A training data set relating to the crack growth was thus obtained. Time segments of vibration signals from a good bearing and a defective one are shown in Figure 8. Their corresponding power spectral densities (PSDs) are shown in Figure 9. The original signals were windowed with each window containing 1000 time points. The maximum values of the vibration signals in each window were also recorded as shown in Figure 10 where x , y , and z represent the three Cartesian axes along which the accelerometer measures the vibrations. The PSDs of the windowed vibration signals were calculated and their peak values extracted as depicted in Figure 11. Figure 12 shows the corresponding crack sizes. Crack size

information at intermediate points was generated via interpolation to avoid a large number of repeated experiments. There are 100 data points for each curve in the figures. The features chosen for prognosis are the maximum signal values and the maximum signal PSDs for all three axes, i.e., (MaxSx MaxSy MaxSz) and (MaxPSDx MaxPSDy MaxPSDz).

Figure 13 demonstrates the crack growth as a function of time. The model was first trained using the fault data up to the 100th time window; from then on, it predicted the crack evolution until the final bearing failure. Mexican hats were used as mother wavelets throughout all the experiments. The virtual sensor, implemented as a WNN with seven hidden nodes or neurons, was trained through the process of Figure 14. This virtual sensor “measured” the crack size on the basis of the maximum signal amplitudes and the maximum signal PSDs as inputs. The training results are depicted in Figure 15. It is observed that 100 data points employed for training led to very satisfactory results. The DWNN, acting as the predictor, was trained next, as shown in Figure 16. The optimized training procedure resulted in a DWNN of 6 input (i.e. the model order is 6), 8 hidden and 2 output neurons. The training took several hours to finish due to a large number of network parameters to be trained, which totaled 368 composed of 6×6×8 for A, 6×8 for B, 2×8 for C and 2×8 for C_{in}. The training results are shown in Figure 17. Training was deemed satisfactory when 100 data points were used. The trained predictor was employed finally to predict the future crack development, as shown in Figure 18. A failure hazard threshold was established on the basis of empirical evidence corresponding to Crack_Width = 2000 microns or Crack_Depth = 1000 microns. The crack reached this hazard condition at the 174th time window. The Crack_Width criterion was reached first. It should be noted that these results are preliminary and intended only to illustrate the proposed prognostic architecture. In practices, a substantially large database may be required for feature extraction, training, validation and optimization. Such a database will permit a series of sensitivity studies that may lead to more conclusive results as to the capabilities and the effectiveness of the proposed approach.

6. CONCLUSIONS

A fault prognostication architecture consisting of a virtual sensor and a dynamic wavelet neural network is proposed. The proposed model addresses two challenging issues relating to prognosis of machine or component failures: How do we “measure” the growth of a fault and how do we predict the remaining useful lifetime of such a failing component or machine? Reliable answers to these questions are bound to assist maintenance personnel in the conduct of condition-based maintenance so that uptime is maximized and the useful life of critical assets is prolonged. Simulation studies of the virtual sensor – predictor configuration, based on a limited experimental data set, show promise. More extensive failure data – difficult to obtain in critical processes – are required to draw firm and comparative conclusions. The proposed architecture provides a generic and open platform that can be easily modified and augmented as new failure evidence becomes available.

ACKNOWLEDGEMENTS

This research was partially supported by Honeywell Inc. and the Office of Naval Research under contract No. E-21-K30. Additional support was provided by the U.S. Navy under an SBIR program. Their assistance in the conduct of this work is greatly appreciated.

REFERENCES

1. Barbera, F., Schneider, H. & Kelle, P.A., “Condition Based Maintenance Model with Exponential Failures and Fixed Inspection Intervals”, *Journal of the Operational Research Society* 47(8), pp. 1037-104, 1996.
2. Frelicot, C., “A Fuzzy-Based Prognostic Adaptive System”, *Journal Europeen des Systemes Automatises* 30(2-3), pp. 281-299, 1996.
3. Groer, P.G., “Analysis of Time-to-Failure with a Weibull Model”, *Proceedings of Maintenance and Reliability Conference (MARCON)*, pp. 59.01-59.04, Knoxville TN, 2000.
4. He, S.C. and He, Z.Y., “Blind Equalization of Nonlinear Communication Channels using Recurrent Wavelet Neural Networks”, *Proceedings of IEEE International Conference on Acoustics, Speech, and Signal Processing*, pp. 3305-3308, 1997.
5. Jardim-Goncalves, R., Martins-Barata, M., Alvaro Assis-Lopes, J. and Steiger-Garcia, “Application of Stochastic Modeling to Support Predictive Maintenance for Industrial Environments”, *Proceedings of IEEE International Conference on Systems, Man and Cybernetics, Information Intelligence and Systems*, pp. 117-122, 1996.
6. Konrad, H. and Isermann, R., “Diagnosis of Different Faults in Milling using Drive Signals and Process Models”, *Proceedings of the 13th IFAC World Congress, Vol.B*, pp. 91-96., 1996.
7. Lembessis, E., Antonopoulos, G., King, R.E., Halatsis, C. and Torres, J., “CASSANDRA: An On-line Expert System for Fault Prognosis”, *Proceedings of the 5th CIM Europe Conference on Computer Integrated Manufacturing*, pp. 371-377, 1989.

8. Makis, V., Jiang, X. and Jardine, A.K.S., "A Condition-Based Maintenance Model", *IMA Journal of Mathematics Applied in Business and Industry* 9(2), pp. 201-210, 1998.
9. Marko, K.A., James, J.V., Feldkamp, T.M., Puskorius, C.V., Feldkamp, J.A. and Roller, D., "Applications of Neural Networks to the Construction of "Virtual" Sensors and Model-Based Diagnostics", *Proceedings of ISATA 29th International Symposium on Automotive Technology and Automation*, pp. 133-138, 1996.
10. Mylaraswamy, D. and Venkatasubramanian, V. , "A Hybrid Framework for Large Scale Process Fault Diagnosis", *Computers & Chemical Engineering* 21(Supplemental Issue), pp. 935-940, 1997.
11. Parker, B.E., Jr., Nigro, T.M., Carley, M.P., Barron, R.L., Ward, D.G., Poor, H.V., Rock, D. and DuBois, T.A., "Helicopter Gearbox Diagnostics and Prognostics using Vibration Signature Analysis", *Proceedings of SPIE - The International Society for Optical Engineering*, Vol.1965, pp. 531-542, 1993.
12. Prickett, P. and Eavery, S., "The Case for Condition Based Maintenance", *Integrated Manufacturing Systems* 2(3), pp. 19-24, 1991.
13. Rao, S.S. and Kumthekar, B., "Recurrent Wavelet Networks", *Proceedings of IEEE International Conference on Neural Networks*, pp. 3143-3147, 1994.
14. Ray, A. and Tangirala, S., "Stochastic Modeling of Fatigue Crack Dynamics for On-line Failure Prognostics", *IEEE Transactions on Control Systems Technology* 4(4), pp. 443-45, 1994.
15. Schauz, J.R. "Wavelet Neural Networks for EEG Modeling and Classification." *PhD Thesis*, Georgia Institute of Technology, 1996.
16. Shiroishi, J., Li, Y., Liang, S., Kurfess, T. and Danyluk, S., "Bearing Condition Diagnostics via Vibration and Acoustic Emission Measurements", *Mechanical Systems and Signal Processing* 11(5), pp. 693-705, 1997.
17. Taylor, N.B. *Stedman's Medical Dictionary*, 18th Edition, The Williams & Wilkins Company, Baltimore, 1953.
18. Tsui, F.C., Sun, M.G., Li, C.C. & Scلابassi, R..J., "A Wavelet Based Neural Network for Prediction of ICP Signal", *Proceedings of IEEE 17th Annual Conference on Engineering in Medicine and Biology and 21st Canadian Conference on Medical and Biological Engineering*, pp. 1045-1046, 1995.

Table 1 Statistical summary of the prognosis for the three retraining cases

Retraining	Max-sum	Min-sum	Mean-sum	Median-sum	STD-sum
0%	36.3343	10.6000	22.2808	21.8376	8.4170
100%	31.5005	3.8809	15.0437	13.8941	8.9190
67%	32.2762	3.6422	15.0822	13.7477	9.1208

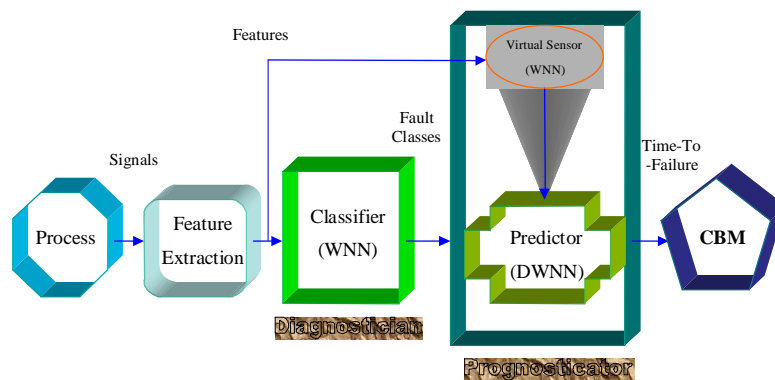


Figure 1. The overall architecture of the prognostic system

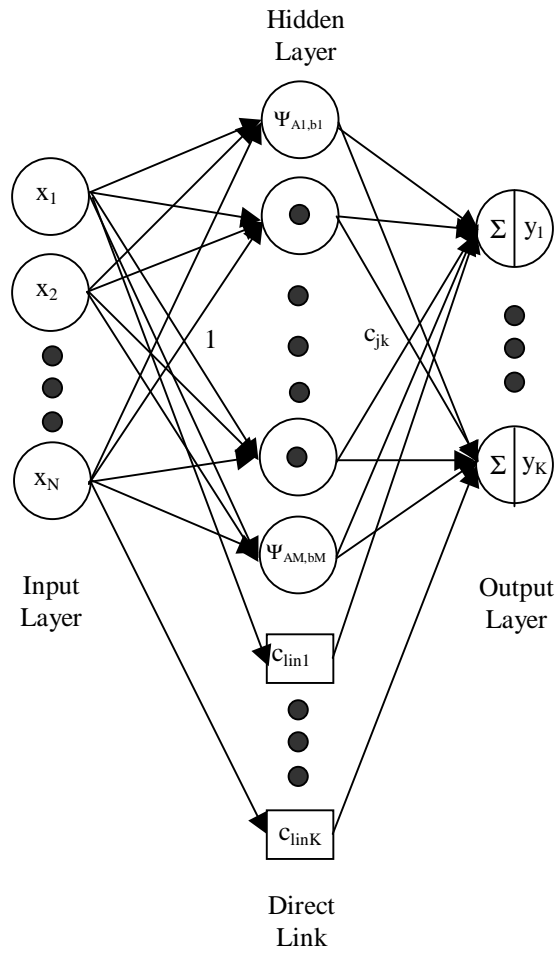


Figure 2. A WNN

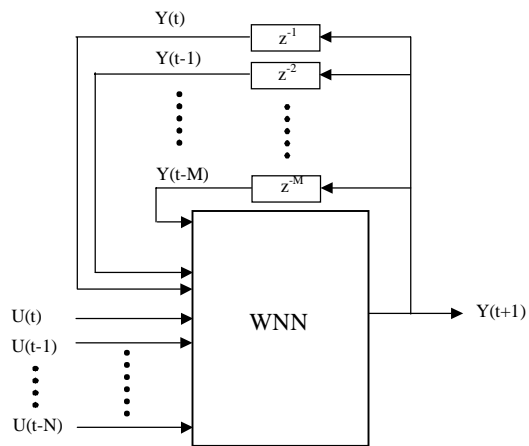


Figure 3. A DWNN

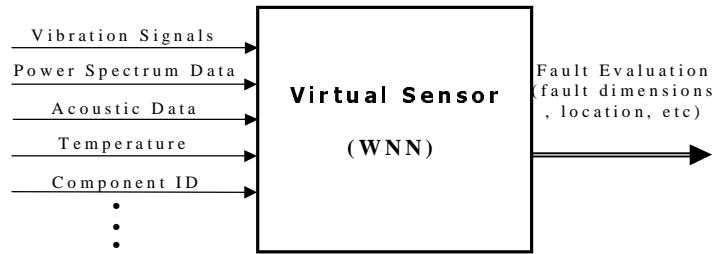


Figure 4. A schematic representation of the WNN as a virtual sensor

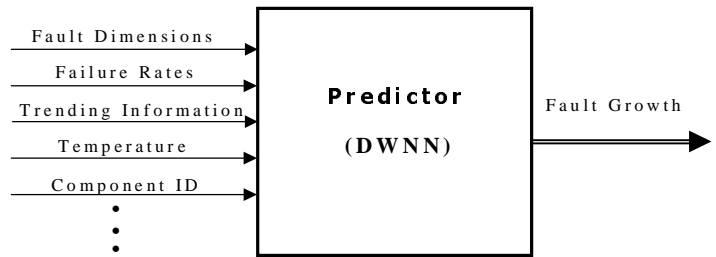


Figure 5. A schematic representation of the DWNN as the predictor

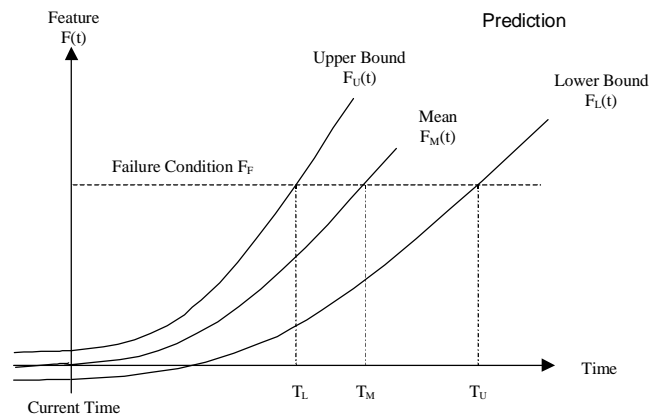


Figure 6. Uncertainty boundaries in a prognostic task

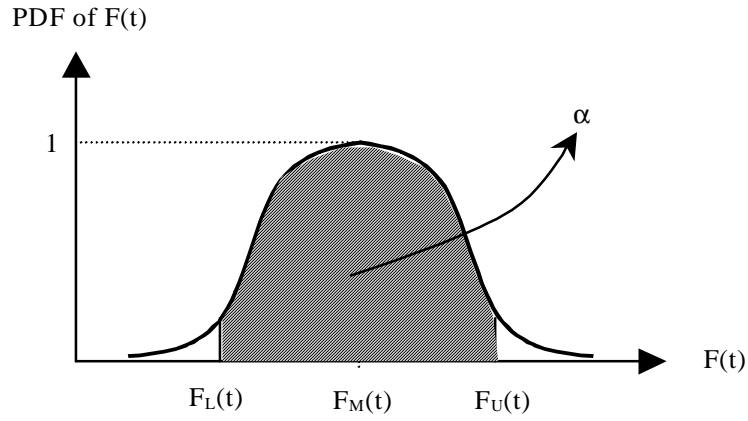


Figure 7. An uncertainty interval with α -level confidence

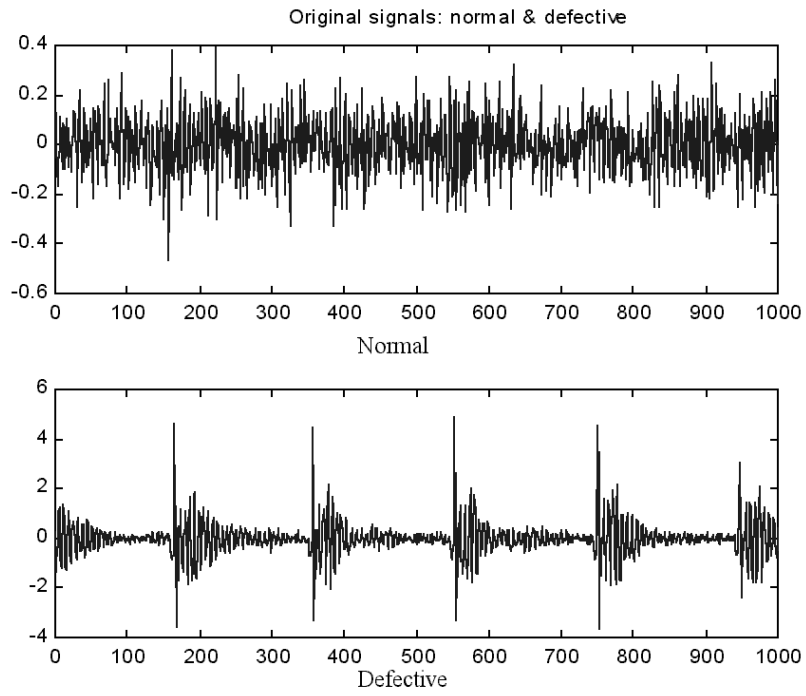


Figure 8. Vibration Signals from a normal and a defective bearing

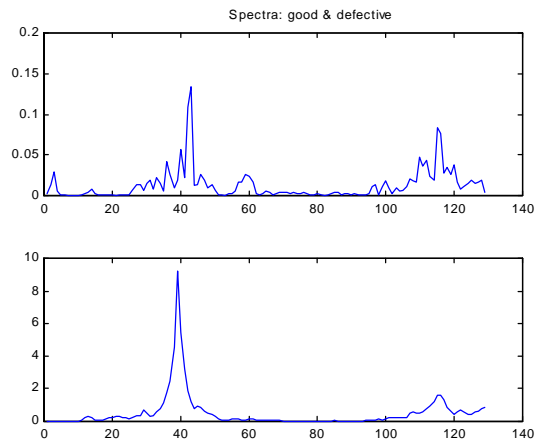


Figure 9 PSDs of the vibration signals in Figure 8

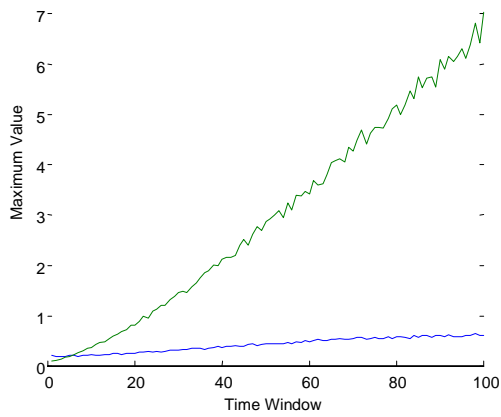


Figure 10 The peak values of the original signals

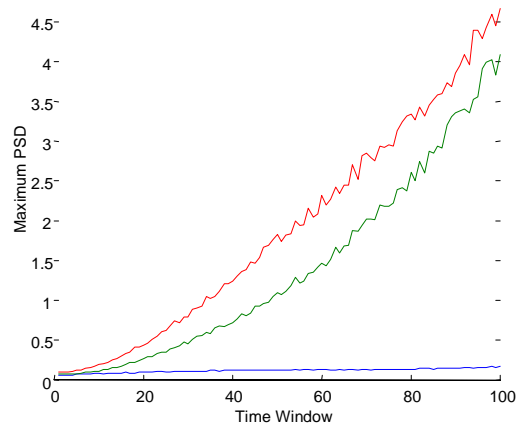


Figure 11 The maximum PSDs of the original signals

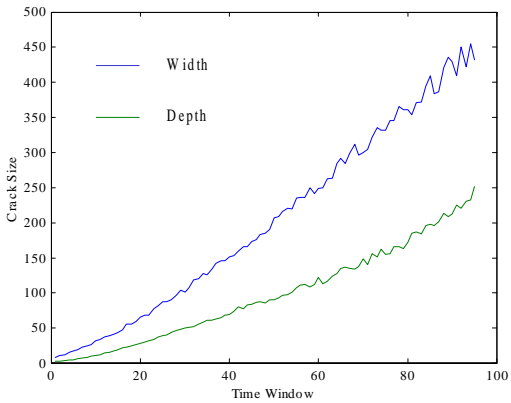


Figure 12 The original crack sizes

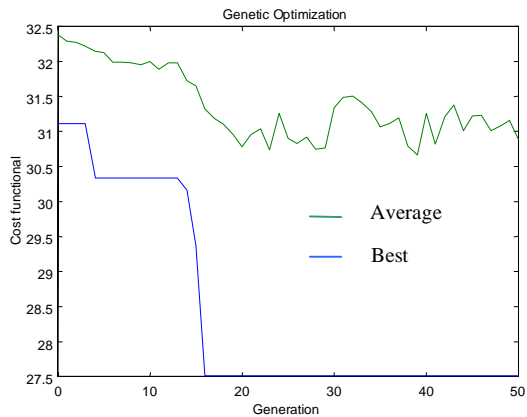


Figure 13 The training of the virtual sensor

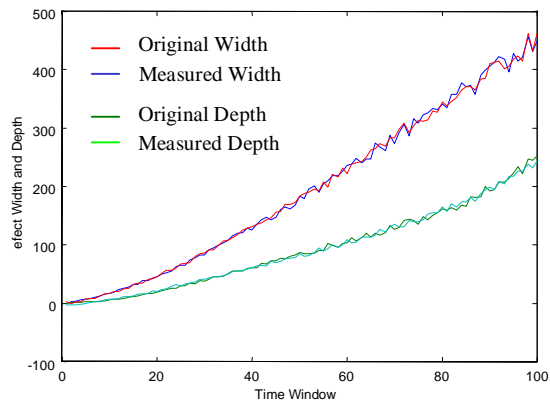


Figure 14 The crack sizes measured by the trained virtual sensor

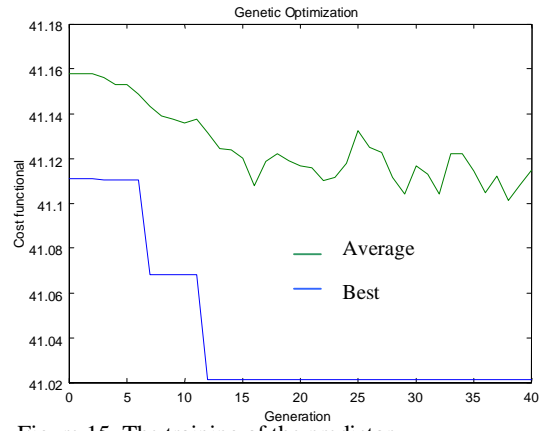


Figure 15 The training of the predictor